Rer1p maintains ciliary length and signaling by regulating γ-secretase activity and Foxj1a levels

Nathalie Jurisch-Yaksi,[1,2] Applonia J. Rose,[1,2] Huiqi Lu,[1,2] Tim Raemaekers,[1,2] Sebastian Munck,[1] Pieter Baatsen,[1] Veerle Baert,[1,2] Wendy Vermeire,[1,2] Suzie J. Scales,[5] Daphne Verleyen,[3] Roel Vandepoel,[3] Przemko Tylzanowski,[3] Emre Yaksi,[4,6] Thomy de Ravel,[7] H. Joseph Yost,[8] Guy Froyen,[1,2] Cammon B. Arrington,[8] and Wim Annaert[1,2]

[1]VIB Center for the Biology of Disease, [2]Center for Human Genetics, [3]Department of Musculoskeletal Sciences, and [4]Department of Neurophysiology, KULeuven, 3000 Leuven, Belgium
[5]Department of Molecular Biology, Genentech, South San Francisco, CA 94080
[6]VIB Neuroelectronics Research Flanders, 3001 Leuven, Belgium
[7]Center for Human Genetics, University Hospitals Leuven, 3000 Leuven, Belgium
[8]Department of Neurobiology and Anatomy, The University of Utah, Salt Lake City, UT 84132

Cilia project from the surface of most vertebrate cells and are important for several physiological and developmental processes. Ciliary defects are linked to a variety of human diseases, named ciliopathies, underscoring the importance of understanding signaling pathways involved in cilia formation and maintenance. In this paper, we identified Rer1p as the first endoplasmic reticulum/cis-Golgi–localized membrane protein involved in ciliogenesis. Rer1p, a protein quality control receptor, was highly expressed in zebrafish ciliated organs and regulated ciliary structure and function. Both in zebrafish and mammalian cells, loss of Rer1p resulted in the shortening of cilium and impairment of its motile or sensory function, which was reflected by hearing, vision, and left–right asymmetry defects as well as decreased Hedgehog signaling. We further demonstrate that Rer1p depletion reduced ciliary length and function by increasing γ-secretase complex assembly and activity and, consequently, enhancing Notch signaling as well as reducing Foxj1a expression.

Introduction

Although primary quality control in the ER accompanies folding and translocation of all proteins in the ER, some proteins, like subunits of protein complexes, require secondary quality control for proper complex assembly (Ellgaard and Helenius, 2003). Rer1p acts in the secondary quality control of several exported and ER-resident proteins and in proper assembly of multimeric complexes (Sato et al., 2004). In mammals, Rer1p interacts with Nicastrin, a component of the γ-secretase complex (Spasic et al., 2007) that governs intramembranous proteolysis of >90 substrates (De Strooper and Annaert, 2010). Two prominent substrates are the amyloid precursor protein, of which the Aβ fragment is central in Alzheimer's disease pathology, and Notch, a key protein in cell fate determination, whose malfunctioning is implicated in several human genetic disorders and cancers (Kopan and Ilagan, 2009). Notch cleavage by γ-secretase releases the Notch intracellular domain (ICD; NICD) to permit its nuclear translocation and activation of target genes (De Strooper et al., 1999). By competing with Aph1 for binding to Nicastrin, Rer1p negatively regulates γ-secretase complex assembly during ER–Golgi recycling (Spasic et al., 2007); however, the physiological consequences of this regulation have remained elusive.

Using a loss of function approach in zebrafish and mammalian cell models, we demonstrate now that Rer1p expression levels regulate cilia length and function. Cilia are evolutionarily conserved organelles emanating from the surface of most vertebrate cells that act in many physiological and developmental processes through generating fluid flow (motile cilia) or transducing signaling pathways (primary cilia), including Hedgehog (Hh), Wnt, and planar cell polarity (Nigg and Raff, 2009).

N. Jurisch-Yaksi and A.J. Rose contributed equally to this paper.

Correspondence to Wim Annaert: Wim.Annaert@cme.vib-kuleuven.be

Abbreviations used in this paper: 5′mmC, 5′ mismatch control; ALL, anterior lateral line; CMV, cytomegalovirus; DFC, dorsal forerunner cell; dpf, day postfertilization; ERG, electroretinogram; FAM, fluorescein; Hh, Hedgehog; hpf, hour postfertilization; ICD, intracellular domain; IFT, intraflagellar transport; KV, Kupffer's vesicle; LR, left–right; MO, morpholino; NICD, Notch ICD; OV, otic vesicle; PLL, posterior lateral line; RPE, retinal pigmental epithelial; SMO, splice-modifying MO; WISH, whole mount in situ hybridization.

The Rockefeller University Press $30.00
J. Cell Biol. Vol. 200 No. 6 709–720
www.jcb.org/cgi/doi/10.1083/jcb.201208175

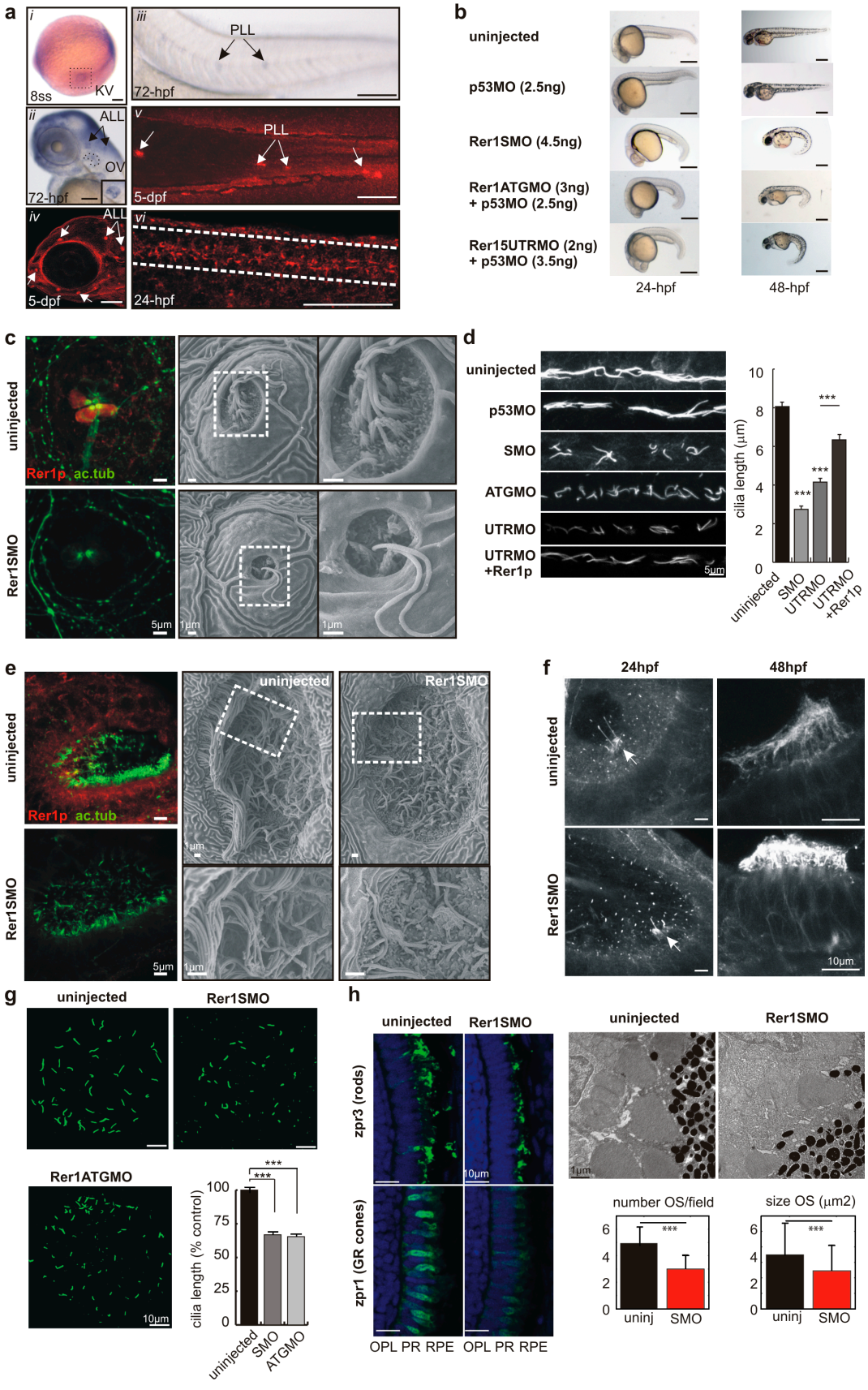

Figure 1. **Rer1p is highly expressed in ciliated organs and affects ciliogenesis in zebrafish.** (a) WISH (*i–iii*) and immunostaining (*iv–vi*) show that *rer1* is highly expressed in ciliated organs: KV (delineated with a dashed box in *i*), lateral views of the otic vesicle (OV; different hybridization probe in inset; *ii*), ALL and PLL neuromasts (*ii–v*), and pronephros (delineated with dashed lines in *vi*). (b) Rer1p knockdown results in a "curly tail down" phenotype after

Ciliary dysfunction, e.g., caused by mutations in ciliary/basal body proteins, gives rise to human syndromes termed ciliopathies. The length of the cilium, which is critical for proper function (Lai et al., 2011), is dynamically controlled through balanced antero- and retrograde ciliary transport governed by, e.g., the intraflagellar transport (IFT) and Bardet–Biedl syndrome protein complexes as well as motor proteins (Ishikawa and Marshall, 2011). Additionally, ciliogenesis is dependent on membrane trafficking from the trans-Golgi network and likely via Rab11-Rab8 exocyst endosomal transport regulation (Feng et al., 2012; He et al., 2012). Thus far, the early biosynthetic compartments, including ER and intermediate compartment, have not yet been implicated in cilia regulation. Here, we identify Rer1p as the first ER–cis-Golgi transmembrane protein involved in motile and primary cilia maintenance and function in zebrafish and mammalian cells. Rer1p exerts this function through controlling γ-secretase activity levels and Notch signaling as well as through transcriptional control of Foxj1a.

Results and discussion

Rer1p is highly expressed in ciliated organs and affects ciliogenesis in zebrafish

To establish the physiological role of Rer1p, we examined its expression pattern and the effect of its knockdown in zebrafish, whose single *rer1* orthologue is 66% identical at the protein level to a human's. From early developmental stages, *rer1* was expressed in ciliated organs, including the Kupffer's vesicle (KV; eight-somite stage), the pronephros (24 h postfertilization [hpf]), the otic vesicle (OV; 72 hpf), olfactory pits (72 hpf), and neuromasts of both anterior lateral line (ALL) and posterior lateral line (PLL; 72 hpf and 5 d postfertilization [dpf]; Fig. 1 a). As this suggests a potential role for Rer1p in cilia formation and function, we next down-regulated *rer1* in zebrafish by injecting either a splice-modifying morpholino (MO; SMO) or two independent translation-blocking MOs (ATGMO or UTRMO). Knockdown efficiency (∼50%) was verified by RT-PCR and Western blotting (Fig. S1, a and b). All MO, but not a 5′ mismatch control (5′mmC) MO, induced a bent body axis with a downward-curved tail (Fig. 1 b and not depicted) characteristic of embryos with defective cilia (Omori et al., 2008). Knockdown of *rer1* led to significant shortening of cilia in all investigated ciliated tissues, as indicated by acetylated tubulin staining and scanning EM of the neuromasts, pronephros, olfactory pits, sensory patch of the inner ear, and KV (Fig. 1 c–g). Importantly, reexpression of Rer1p could rescue the length of pronephric cilia (Fig. 1 d). In addition, the connecting cilia of the photoreceptor outer segment were impaired in 4-dpf Rer1p morphants, as indicated by lesser number and size by transmission EM and diminished rods (zpr3) and green–red cones (zpr1) in retinal cryosections (Fig. 1 h). The pronounced ciliary phenotypes persisted over a range of developmental stages (e.g., for OV at 24 and 48 hpf; Fig. 1 f) and thus are not caused by developmental delay.

Functional impairment of the ciliated organs in Rer1p morphant embryos

We next investigated whether the observed structural defects resulted in aberrant organ physiology. The formation of otoliths, which are calcium-carbonate crystals located in the zebrafish inner ear, critically depends on the ciliated sensory epithelium. Wild-type zebrafish have one large (posterior) and one small (anterior) otolith (Whitfield et al., 2002), but Rer1p morphants exhibit abnormal otolith number, size, and positioning (Fig. 2 a), likely resulting from defective OV ciliary structure. The ciliated epithelium of the inner ear also has an auditory function, and Rer1p depletion prevented responses to acoustic stimuli (Videos 1 and 2) in the acoustic startle reflex test (Sidi et al., 2003). In line with the morphological defects observed in the retina, the optokinetic behavior response, which measures the visual acuity of the larvae, was also reduced or even absent in Rer1p morphants (Fig. 2 b) and electroretinograms (ERGs) revealed a threefold reduction in photoreceptor electrical activity (Fig. 2 c).

Left–right (LR) patterning and heart looping in zebrafish relies upon the function of motile cilia in the KV. Herein, the movement of cilia creates a unidirectional fluid flow resulting in asymmetrical gene expression important for the LR orientation of many organs (Essner et al., 2005; Kramer-Zucker et al., 2005). Fluorescent beads injected into the KV lumen of uninjected embryos moved briskly and counter clockwise, but in Rer1p morphants with shortened cilia, they merely resembled Brownian motion (Fig. 2 d and Videos 3 and 4). Impaired cilia-driven fluid flow likely explains the LR asymmetry defects, reflected by randomization or loss of the expression patterns of *lefty1* and *lefty2* (Fig. 2 e) and reversal or absence of heart looping (Fig. 2 f) observed in morphants. Importantly, the function of Rer1p in KV is cell autonomous, as the injection of either ATGMO or UTRMO specifically in KV precursors (dorsal forerunner cells [DFCs]) lead to randomization of *lefty2* expression (Fig. 2 e).

The development of the craniofacial skeletal elements is also dependent on functionally intact cilia (Zaghloul and Brugmann, 2011). Interestingly, Rer1p morphants had defects in the pectoral fin cartilage (not depicted) and abnormal head skeletal features

24 hpf. (c) Ciliary defects in SMO ALL neuromast cells at 48 hpf (confocal) and 72 hpf (scanning EM; zoomed area of boxes in right images). Rer1p staining is absent in SMO. (d) Pronephric cilia are shortened in Rer1p morphants (SMO, ATGMO, and UTRMO) compared with control (uninjected and p53MO) and rescued upon reexpression of Rer1p ($n > 9$; three experiments). (e) Ciliary defects of olfactory pits in SMO at 48 hpf (confocal; scanning EM). Boxed areas are enlarged in the bottom images. (f) Short cilia in the inner ear sensory patches of SMO at 24 hpf (indicated with arrows) and 48 hpf. (g) Reduced cilia length in the KV (10-somite stage [ss]) of SMO/ATGMO ($n = 10$). (h, left) Impaired photoreceptor outer segments (OS) in 4-dpf SMO. OPL, outer plexiform layer; PR, photoreceptor; RPE, retinal pigment epithelium. (right) EM of OS of 4-dpf larvae. Decreased number and mean size of the outer segments in SMO ($n = 4$ embryos). uninj., uninjected. In all panels except h, cilia are visualized using anti–acetylated tubulin (ac.tub) staining. Means ± SD (h) or SEM (d and g); ***, $P < 0.001$, Wilcoxon rank sum test (h) or Student's *t* test (d and g). Bars: (a) 100 µm; (b) 500 µm.

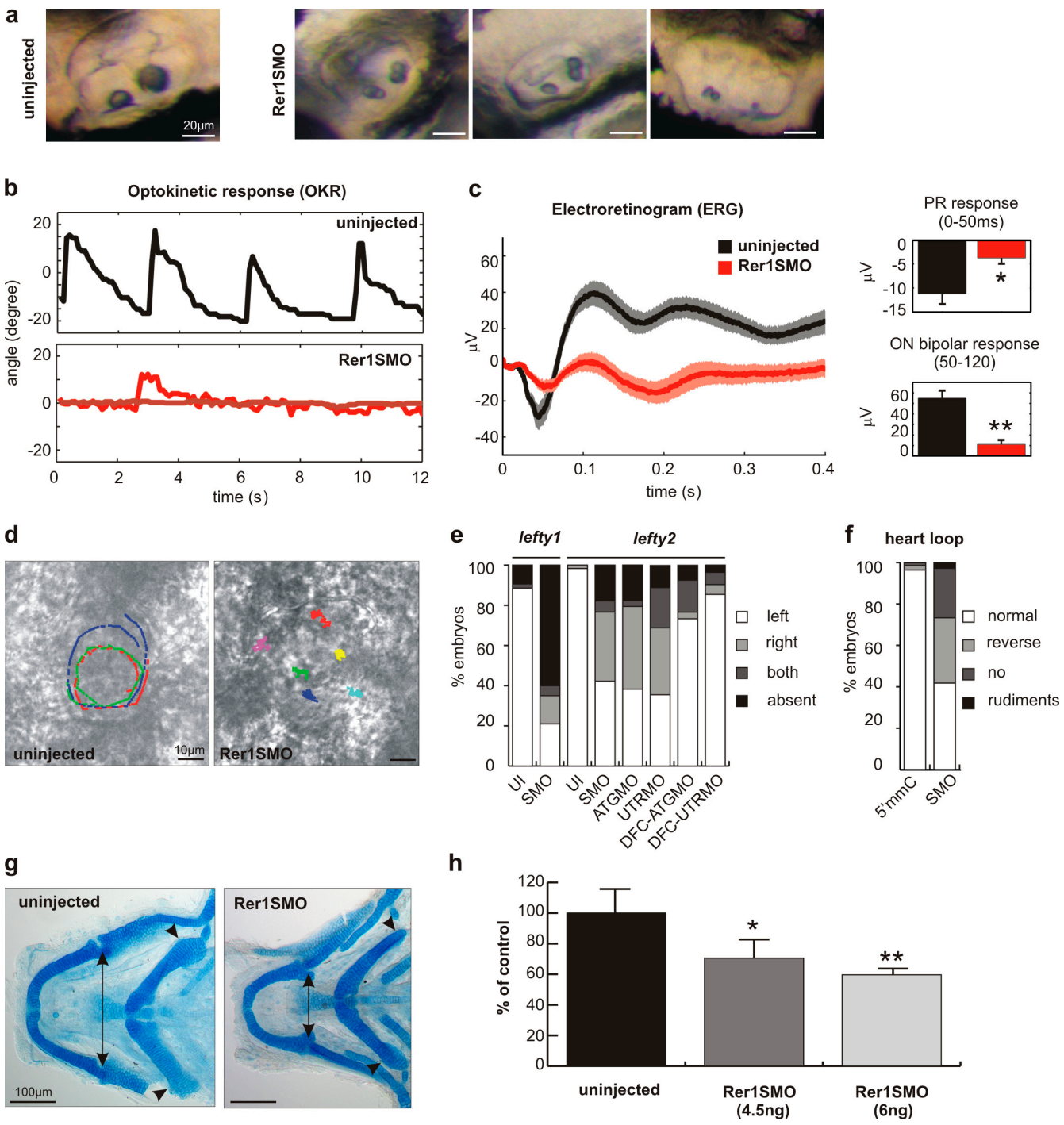

Figure 2. **Functional impairment of the ciliated organs in Rer1p morphant embryos.** (a) Defective otolith formation in the inner ear of SMO. (b) Reduced or absent optokinetic response of 4.5-dpf SMO. The relative angle of eye rotation is shown for a control and two SMO larvae ($n > 10$). (c) Impaired retinal activity as measured by ERG in 4.5-dpf SMO; mean ± SEM is represented by shading. Decreased photoreceptor (PR) response and concomitant ON bipolar response ($n \geq 16$). (d) Directional fluid flow in the KV is absent in the SMO as shown by fluorescent bead tracking (see Videos 3 and 4). Colored tracks show individual bead movements. (e) Randomization or loss of expression of Nodal antagonists *lefty1* and *lefty2* in SMO, ATGMO, and UTRMO as well as in DFC-specific injection of ATGMO and UTRMO at 20 hpf. Bars indicate percentages of embryos with expression on either side, both sides, or absent ($n \geq 90$). UI, uninjected. (f) Reversal or absence of heart looping in SMO at 48 hpf. Bars indicate percentages of normal, reverse, or no heart looping. (g) Dorsal view of Alcian-stained cartilage of zebrafish heads. Arrowheads point to changes in pharyngeal cartilage chondrocyte number/arrangement; morphometric differences indicated by arrows are quantified in h. Means ± SEM (c) or SD (h); *, $P < 0.05$; **, $P < 0.01$, Wilcoxon rank sum test (c) or Student's *t* test (h).

seen as a change in pharyngeal cartilage chondrocyte number and arrangement (Fig. 2 g) as well as morphometric changes in the mandibular cartilage (Fig. 2 h). Collectively, these findings demonstrate that Rer1p affects not only the length but, very importantly, the function of both motile and primary cilia in zebrafish in a cell-autonomous fashion.

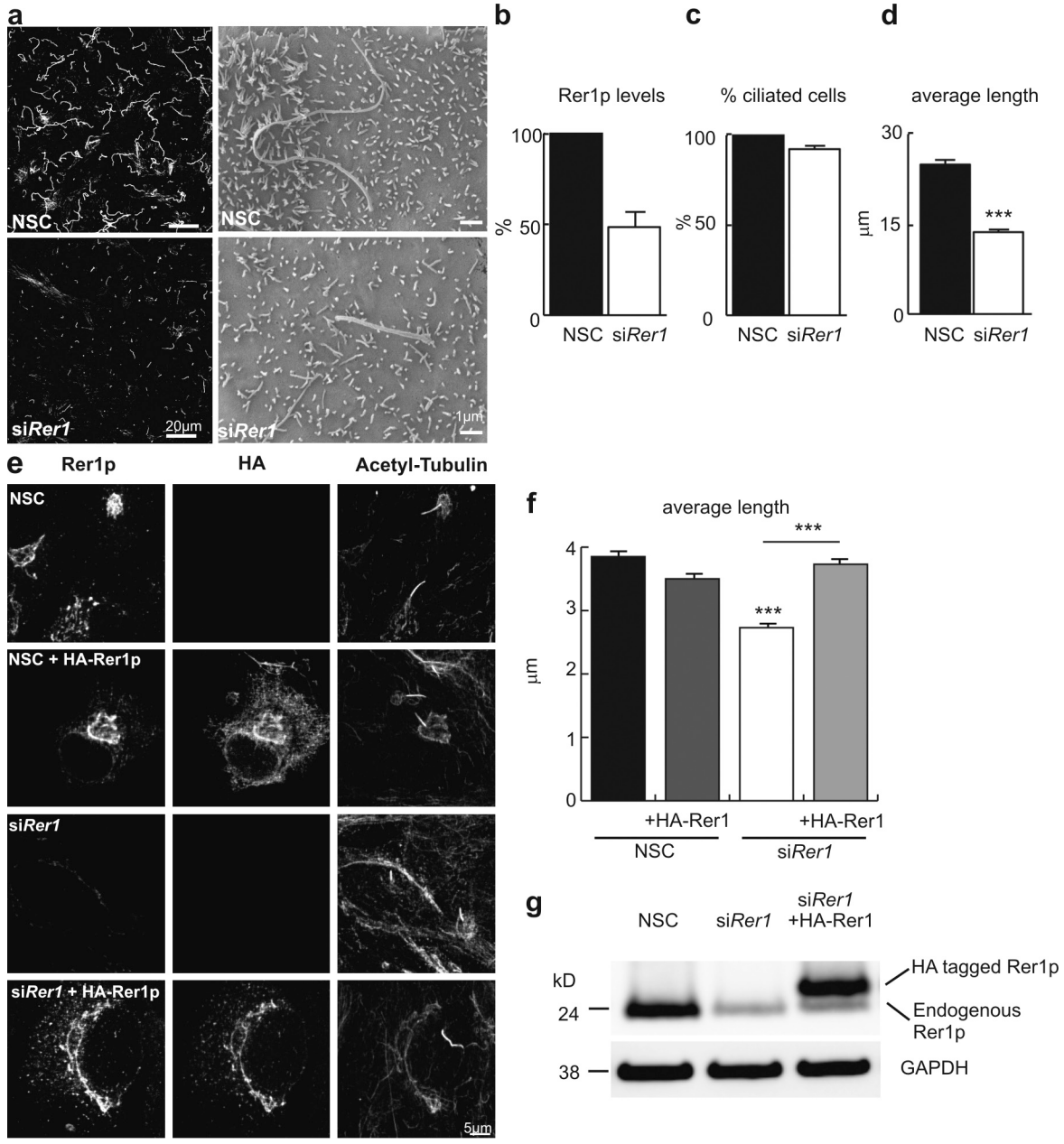

Figure 3. **The regulatory role of Rer1p in cilia formation is conserved in mammalian cells.** (a) Anti–acetylated tubulin staining and scanning EM demonstrates shorter cilia after *rer1* knockdown in CL4 cells. (b) Efficiency of *rer1* knockdown by RNAi (si*Rer1*) in CL4 cells compared with nonspecific control (NSC) using at least three Western blots (normalized to GAPDH). (c) Unaffected number of ciliated cells upon *rer1* knockdown in CL4. (d) Twofold decrease in mean cilia length upon *rer1* knockdown in CL4 ($n > 684$). (e) Shorter cilia after *rer1* down-regulation in RPE cells are rescued upon reexpression of HA-tagged Rer1p. Western blot is shown in g. Quantification ($n \geq 95$) shown in f. Means ± SEM (d and f) or SD (b). ***, $P < 0.001$, Wilcoxon rank sum test.

The regulatory role of Rer1p in ciliogenesis is conserved in mammalian cells

We next turned to in vitro cell models such as porcine kidney (CL4) and human retinal pigmental epithelial (RPE) cells, both commonly used for studying cilia. Knockdown of *rer1* using RNAi silencing in CL4 had no effect on cilia number but significantly decreased mean cilia length to 58 ± 4% of control (Fig. 3, a–d). Similar results were obtained upon *RER1* down-regulation in RPE cells and could be rescued upon reexpression of Rer1p (Fig. 3, e–g), thereby implying a conserved role of Rer1p in the maintenance of cilia in cell culture. Importantly, Rer1p regulates cilia length cell autonomously because depleted cells adjacent to rescued cells still displayed a short cilium (Fig. 3, e and f).

We next investigated whether the Hh signaling pathway, which depends on intact primary cilia (Huangfu et al., 2003; Eggenschwiler and Anderson, 2007; Lai et al., 2011), was affected upon *rer1* down-regulation by using an Hh-responsive reporter assay in S12 cells (Frank-Kamenetsky et al., 2002). Down-regulation of *rer1* decreased Hh signaling (55 ± 6% of control; Fig. 4 a) similar to that of knockdown of Ift88, a ciliary transport machinery protein. We next investigated whether

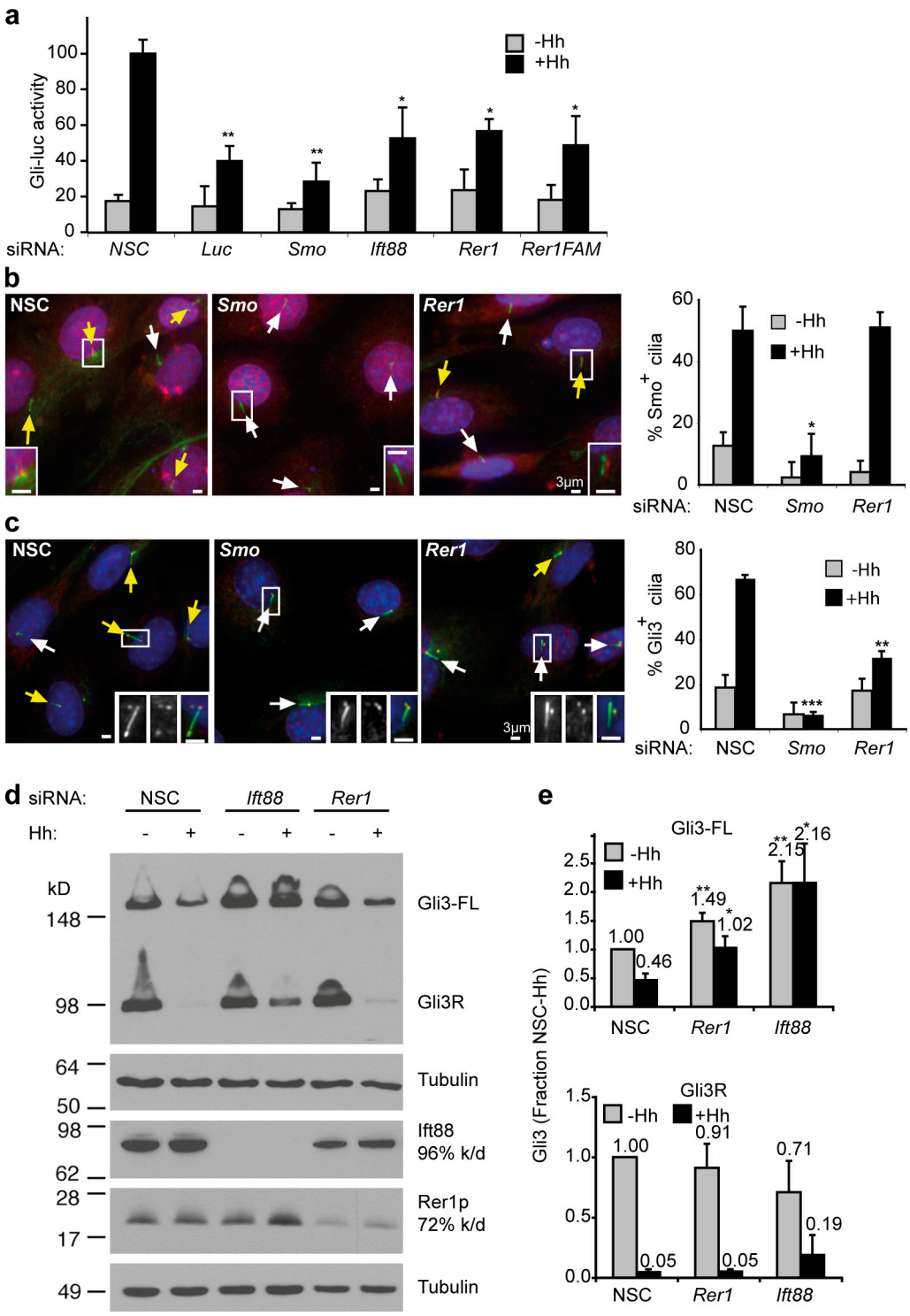

Figure 4. **Rer1p knockdown in S12 cells decreases Hh signaling.** (a) *Gli* luciferase reporter assay reveals that Rer1p depletion inhibits Hh signaling similarly to Ift88 knockdown but less than depletion of Smoothened (Smo) or luciferase (Luc); Rer1F is a FAM-labeled Rer1 siRNA. NSC, nonspecific control. (b, left) Smoothened is transported normally to the cilia of Rer1p-deficient cells after 21-h Hh stimulation. (insets) Magnification of boxed areas with the red Smoothened channel displaced six pixels to the right. Arrows point to tips of cilia: white for Smoothened$^-$ and yellow for Smoothened$^+$ cilia. (right) Quantification of Smoothened translocation to cilia. (c, left) Rer1p inhibits ciliary accumulation of Gli3 (red). Arrows point to cilia tips: white for Gli3$^-$ and yellow for Gli3$^+$ cilia. (right) Quantification of Gli3 accumulation at cilia tips. (b and c, insets) Bars, 3 µm. (d) Hh-dependent Gli3 degradation, but not processing, is inhibited by Rer1 depletion. (e) Representative Western blot and quantification (n = 4 independent experiments) of Gli3FL and Gli3R normalized to tubulin. Acetylated and γ-tubulin are shown in green, and DAPI is shown in blue (b and c). Represented are means ± SD of more than three experiments. *, $P \leq 0.05$; **, $P \leq 0.01$ by Student's t test.

ciliary trafficking of key players of the pathway was also disturbed. Rer1p depletion did not affect the Hh-dependent ciliary accumulation of the signal transducing protein Smoothened (Fig. 4 b) but did inhibit that of Gli3 (Fig. 4 c), which is essential for its activation and lability (Wen et al., 2010). In accordance with this, Hh-dependent Gli3FL degradation was impaired, with a concomitant increase in baseline Gli3FL levels. There was no impact on Gli3 processing into Gli3R, which only occurs in the absence of Hh (Fig. 4, d and e). Collectively, these data suggest that Rer1p acts between Smoothened and the Gli transcription factors, the same step of the Hh pathway that is regulated by other ciliary proteins (Huangfu et al., 2003). Reduced Hh signaling in *Rer1*-depleted cells is thus probably secondary to the ciliary defects and implies that Rer1p regulates the length and thereby the function of the primary cilium.

Reduced cilium length is caused by enhanced γ-secretase activity and diminished Foxj1a levels

Given Rer1p's role in Golgi to ER recycling and complex formation, it could regulate cilia length by controlling vesicular trafficking toward cilia or the assembly of protein complexes critical for ciliogenesis. To test this, we monitored the trafficking and expression levels of core ciliary membrane components (polyductin and polycystin), proteins controlling vesicular transport toward and within cilia (BBS4, BBS7, Rab8, Arl13b, IFT20, and GMAP210) or components of the IFT machinery (Kif3a). Rer1p depletion did not prevent the localization of any of these components to the shortened cilia nor did it significantly affect their total cellular levels (Fig. S2), thereby ruling out a direct role for Rer1p in the ER–Golgi transport and sorting of major ciliary membrane or transport complexes.

We therefore investigated whether its previously identified function in regulating γ-secretase activity (Spasic et al., 2007) could be responsible for the observed cilia defects. We first confirmed elevated γ-secretase activity in *Rer1*-depleted CL4 cells by monitoring the processing of NotchΔE (Notch without its extracellular domain), the direct substrate for γ-secretase, into NICD (2.5 ± 0.5–fold of control; Fig. 5 a). Then, we mimicked elevated γ-secretase activity in CL4 cells by overexpressing the ICD of some of its substrates and monitored cilium length. Overexpressing NICD, but not Cadherin ICD, resulted in significant shorter cilia (Fig. 5 b), suggesting that a gain of function of γ-secretase–mediated processing of Notch may cause a detrimental effect on cilia length. This instigated us to determine whether inhibiting γ-secretase activity would rescue the ciliary phenotype in Rer1p down-regulated cells. To avoid full blockade of γ-secretase activity, we titrated low doses of inhibitor X (L685,458) in the range of its known half-maximal inhibitory concentration (of 17 ± 8 nM; Shearman et al., 2000). Interestingly, the reduced cilia length in Rer1p down-regulated CL4 cells was dose-dependently rescued with 5–15 nM of the inhibitor while not affecting cilia length in control cells (Fig. 5 c). Collectively, these data suggest a causal relationship between decreased levels of Rer1p, increased γ-secretase activity, Notch signaling, and maintenance of ciliary length and thus function.

To substantiate the relevance of our findings in cell models, we investigated whether γ-secretase and Notch signaling were also enhanced in Rer1p morphant embryos. Whole mount in situ hybridization (WISH) revealed reduced levels of the Notch ligand and target gene *deltaA*, whereas the expression of *deltaD*, *jagged1*, *jagged2*, *notch1*, and *notch3* were unaffected by Rer1p depletion (Fig. 5 d and not depicted). Next, using a Notch reporter transgenic line (Tp1:hmgb1-mCherry; Parsons et al., 2009), we observed a significant 1.4-fold increase in fluorescence signal in the ear sensory patch of morphants (Fig. 5 e). A similar increase was observed in other organs that express Rer1p but not in the tail tip where Rer1p is not enriched (Fig. 5 e). The lower levels of *deltaA* and the increased Notch reporter signal suggest that, in zebrafish, loss of Rer1p increases γ-secretase activity and Notch signaling.

Differentiation of sensory hair cells in zebrafish depends on Notch signaling: inhibition of Notch increases the production of hair cells (Haddon et al., 1998), whereas its overactivation inhibits their differentiation (Daudet and Lewis, 2005). We addressed whether the ciliary defects in hair cells may be subsequent to enhanced Notch signaling. Rer1p morphants exhibited not only a 50% reduction of the number of neuromasts (FM1-43 dye labeling; Fig. 5 f) but also a decrease in hair cells per sensory patch to 46 ± 4% of control ET4 transgenic fish (Fig. 5g; Daudet and Lewis, 2005). Similar results were obtained in embryos overexpressing NICD (71 ± 3% of control). Conversely, chemical inhibition of γ-secretase increased the number of hair cells per neuromast (to 147 ± 10%) and rescued morphants to wild-type levels (to 95 ± 8% of control and 203 ± 18% of SMO; Fig. 5 g). Altogether, these data suggest that ciliary defects observed in hair cells may result from impaired differentiation subsequent to enhanced γ-secretase activity and Notch signaling.

Additionally, Notch signaling regulates proper LR determination, as both loss and gain of function in zebrafish result in LR asymmetry defects (Raya et al., 2003; Lopes et al., 2010). More particularly, *deltaD* mutant embryos harbored reduced KV cilia length and diminished levels of the ciliogenic factor *foxj1a* (Yu et al., 2008; Lopes et al., 2010). Because Rer1p morphant embryos displayed similar LR asymmetry defects and KV dysfunction, we analyzed the levels of the ciliogenic transcription factor *foxj1a* in those embryos. Interestingly, *foxj1a* was not detectable in the DFC, KV, and pronephros of Rer1p morphants (Fig. 5, h and i). Unaffected levels of *lrdr1*, a marker of the DFC lineage, suggest that Rer1p does not affect DFC/KV cellular differentiation but rather is necessary for the correct expression of *foxj1a*. Increased Notch signaling did not interfere with *foxj1a* levels (Fig. 5 i), suggesting that another γ-secretase substrate could regulate *foxj1a*. Alternatively, Rer1p may affect *foxj1a* through a yet unknown route. Notably, reexpression of Foxj1a in morphants could partially rescue KV and pronephros cilium length (Fig. 5, j–l), thereby further strengthening a genetic interaction of Rer1p and Foxj1a in regulating ciliogenesis in zebrafish.

Collectively, these findings imply that Rer1p controls ciliary length and functions cell autonomously through regulating γ-secretase complex assembly (and activity) and consequently Notch signaling as well as Foxj1a expression. These original

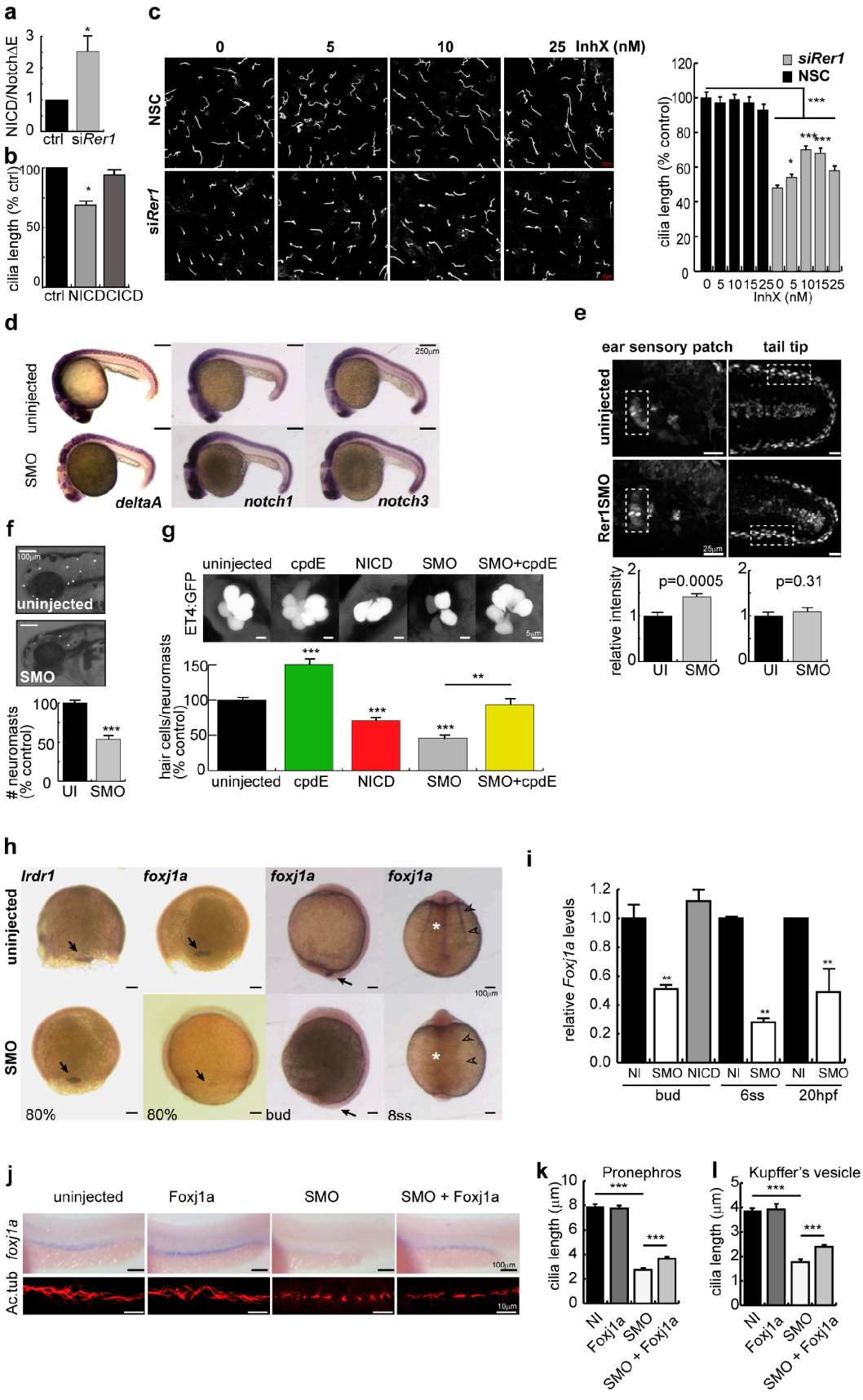

Figure 5. **Reduced cilium length is caused by enhanced γ-secretase activity and diminished Foxj1a levels.** (a) 2.5-fold increased γ-secretase activity in Rer1p-depleted CL4 cells as indicated by increased NICD production ($n = 7$). ctrl, control. (b) Overexpression of NICD but not of Cadherin ICD (CICD) reduces cilium length in CL4 cells. (c) Nanomolar concentrations of γ-secretase inhibition (InhX) rescue cilia length in Rer1p-depleted CL4 cells without

findings markedly expand our understanding of the physiological function of Rer1p in ciliogenesis across in vitro cellular models and in vivo in the zebrafish. Interestingly, so far, no resident integral membrane protein of the early secretory pathway has been functionally associated with ciliogenesis, therefore placing Rer1p as the first ER/cis-Golgi membrane protein involved in ciliogenesis. Here, we show that Rer1p regulates ciliary signaling pathways as early as in pre-Golgi compartments by negatively controlling the assembly of the γ-secretase complex (Spasic et al., 2007), which ultimately exerts its main catalytic function in post-Golgi compartments, rather than by regulating the ER–Golgi transport and sorting of major ciliary complexes. Although some of the cilia defects seem to be dependent on Notch, Foxj1a levels are affected by another mechanism that may involve other γ-secretase substrates or another Rer1p interactor. Thus far, polycystin and polyductin are the only identified ciliary-localized γ-secretase substrates (Pazour et al., 2002; Nauli et al., 2003; Kaimori et al., 2007), but a functional link between their processing and ciliogenesis has not been established. In mammals the only known Rer1p interactor distinct from γ-secretase, the acetylcholine receptor α subunit (Valkova et al., 2011), is expressed principally in the nervous system, and no ciliary function has been associated with it so far. The reason why loss of Rer1p expression emerges most prominently as a ciliopathy is likely related to its higher expression in ciliated cells and organs during development as opposed to adjacent tissues.

In summary, our work highlights the critical importance of balanced γ-secretase activity during development. Altogether, the impact of γ-secretase on ciliary function calls for additional caution in developing γ-secretase–based therapeutics but at the same time encourages greater efforts in exploring its physiological roles.

Materials and methods

Zebrafish lines and injection

Adult wild-type AB as well as ET4 (gift of H. Lopez-Schier, Center for Genomic Regulation, Barcelona, Spain; Parinov et al., 2004) and TP1: hmgb1-mCherry (gift of M. Parsons [Johns Hopkins University, Baltimore, MD] and L. Bally-Cuif [Centre National de la Recherche Scientifique, Gif-sur-Yvette, France]; Parsons et al., 2009) transgenic zebrafish were maintained at 28.5°C under standard aquaculture conditions. All experiments were approved by the Ethics Committee of KULeuven.

2, 3, or 4.5 ng MOs (Gene Tools, LLC) in 1-nl droplets was injected into the yolks of one- to four-cell stage embryos. Where indicated, 5′mmC was used as an additional control for SMO. The sequences of the MOs used (Table S4) were ATGMO (5′-CCGGCACTGTCTCCTTCTGGCATTC-3′), SMO(5′-CCACCCCTAATACAAACAAACAAAC-3′), 5′mmC(5′-CCAgCCgTAATACAAAgAAtCAtAC-3′, lowercase letters represent the mismatches compared with SMO), UTRMO (5′-TCCGGTTGTGCCGCTGTGTCACTTT-3′), and p53MO (5′-GACCTCCTCTCCACTAAACTACGAT-3′).

100 pg of capped NICD or 75 pg of capped Rer1 mRNA was injected into the yolk of one-cell stage embryos. To generate 5′ capped mRNA, linearized DNA was incubated for 20 min at 37°C with 1 mM cap structure, 1 mM ATP, CTP, and UTP, and 0.1 mM GTP and the RNA polymerase SP6 and then for 60 min with an additional 0.5 mM GTP. Template DNA was then digested by the addition of RNase-free DNase for 1 h at 37°C, and the mRNA was purified on a column (Bio-Spin; Bio-Rad Laboratories). Its integrity was verified on an agarose gel.

To target MO specifically to DFCs, 1 nl fluorescein (FAM)-tagged MO (16–24 ng) was injected into the yolk at the 1,000-cell stage. At shield stage, the embryos in which the dye had diffused throughout the yolk and enriched around the germ ring were selected and further analyzed.

Mammalian cell lines, culture conditions, and transfections

LLC-CL4 (CL4 porcine kidney epithelial; gift from J. Bartles, Northwestern University Feinberg School of Medicine, Chicago, IL) cells were maintained in MEM-α medium with 10% FBS and 1% penicillin-streptomycin. RPE (human retinal pigmental cells) were grown in DMEM/F12 with GlutaMAX and 10% FBS. Human embryonic kidney cells were cultured in DMEM/F12 medium plus 10% FBS. S12 cells were maintained in DMEM with 10% FBS and 2 mM L-glutamine. All the cell lines were grown at 37°C in a humidified incubator with 5% CO_2. All cell culture reagents were purchased from Invitrogen/Gibco. To induce primary cilia formation, RPE cells were first cultured to confluency for 48 h in 10% FBS medium and then serum starved (0.5% FBS) for another 48 h.

Down-regulation of Rer1p was achieved using siRNA oligonucleotides. The target sequence 5′-AATATCAGTCCTGGCTAGACA-3′ was used for human *rer1* (for RPE cells), and 5′-CCTGGTGATGTACTTCATCATGCTT-3′ was used for mouse *rer1* (for CL4 and S12 cells). Oligonucleotides (Thermo Fisher Scientific for human *rer1* and Stealth and Invitrogen for mouse *rer1*) were annealed and transfected using Lipofectamine and a reverse transfection protocol, which transfects cells during seeding. The GL2 luciferase RNAi duplex (5′-ACAUCACGUACGCGGAAUACUUCGA-3′) was used as a nonspecific control. In some instances, the oligonucleotides were FAM labeled (AM1634; Ambion) before annealing. Cells were analyzed 72 h (CL4 cells) or 96 h (RPE cells) after transfection with serum starvation (0.5%) for the last 48 h in RPE cells. RNAi against Smoothened (D-041026-01 to -04; Thermo Fisher Scientific), Ift88 (D-050417-01 to -04; Thermo Fisher Scientific), and luciferase as well as control RNAi (nonspecific control; D-001810-10-20; Thermo Fisher Scientific) was performed by 72-h reverse transfection of S12 cells (Gli luciferase C3H10T1/2 mouse osteoblasts) with DharmaFECT 4 (Evangelista et al., 2008; Lai et al., 2011).

For transient overexpression of NICD and N-cadherin ICD, 8 µg of expression vector was used to transfect CL4 cells at 75% confluency, using FuGENE HD (Roche). 48 h after transfection, cells were fixed with 4% PFA and analyzed by immunostaining.

To rescue Rer1p expression in knockdown RPE cells, HA-tagged human Rer1 was cloned into the lentiviral vector, pLA-cytomegalovirus (CMV), and four nucleic acids were mutated in the siRNA targeted region of Rer1 (QuikChange II Site-Directed Mutagenesis kit; Agilent Technologies). Lentivirus was generated in HEK 293T cells by transient cotransfection for 24 h of pLA-CMV-HA-Rer1 and the packaging vectors pCMV-VSVG and pMD2.G using TurboFECT (Thermo Fisher Scientific). RPE cells were reverse transfected with siRNA for 24 h and then infected with lentivirus in the presence of 8 µg/ml polybrene and incubated for a further 72 h, with serum starvation during the last 48 h to promote ciliogenesis. Table S1 provides an overview of the cell lines, and Table S2 provides the siRNAs used.

Gli luciferase assay

The Gli luciferase assay was performed in S12 cells stably transfected with an Hh-responsive *Gli* luciferase reporter containing nine Gli binding sites,

affecting cilia length in control cells. Acetylated tubulin staining ($n = 150$; three experiments). NSC, nonspecific control. (d) Reduced *deltaA* but unaffected *notch1* and *notch3* levels in 24-hpf SMO. (e) Enhanced Notch signaling in the ear sensory patch, but not in the tail, indicated by increased fluorescence of the Notch reporter line Tp1:hmgb1-mCherry. Quantification is shown of highlighted regions ($n > 15$). UI, uninjected. (f) FM1-43 dye labeling shows a twofold reduction in the number of neuromasts in 3-dpf SMO. (g) Twofold reduction in the number of hair cells per neuromast (PLL) in 2-dpf SMO-injected ET4 transgenic embryos. Increased Notch signaling (100 pg NICD mRNA) results in less hair cells per neuromast (71% of control), whereas inhibiting Notch signaling (25 µM compound E [cpdE]) increases hair cell number (150% of control) and rescues the effect of SMO from 46 to 93.6% ($n > 12$). (h) WISH shows normal differentiation of the DFC/KV lineage (*lrdr1*) but reduced *foxj1a* levels in DFC (80% epiboly, arrows), KV (bud, arrows), pronephros (arrowheads), and notochord (asterisks). ss, somite stage. (i) Quantification of *foxj1a* levels by quantitative PCR in SMO. NICD does not affect *foxj1a* levels in the bud. NI, not injected. (j–l) Partial rescue of pronephros (j and k) and KV (l) cilia length upon coinjection of Foxj1a ($n \geq 11$ embryos; three experiments). Ac.tub, acetylated tubulin. Means ± SEM; *, $P < 0.05$; **, $P < 0.01$; ***, $P < 0.001$, Wilcoxon rank sum test (b and c) or Student's *t* test (a, e, g, i, k, and l).

as previously described (Frank-Kamenetsky et al., 2002; Evangelista et al., 2008). In brief, 11,000 S12 cells per well of a 96-well plate were reverse transfected with 100 nM siGenome pools of the indicated murine siRNAs using DharmaFECT #4 (Thermo Fisher Scientific). Cells were incubated for 48 h followed by 24-h serum starvation in 0.5% FBS medium ± 200 ng/ml octyl-Hh (72-h total siRNA transfection). Luciferase levels were assayed with HTS steadylite (PerkinElmer) following the manufacturer's instructions and were measured with a luminometer (TopCount; Applied Biosystems). Cell viability was measured in a parallel plate under the same conditions with a cell viability assay (CellTiter-Glo; Promega) according to the manufacturer's instructions.

γ-Secretase inhibition and activity measurement

γ-Secretase activity was inhibited upon treatment with Inhibitor X (L-685,458; EMD Millipore) in cell culture. The inhibitor was added 3 h after seeding and replaced every 24 h. 25 µM compound E (EMD Millipore) was used for zebrafish experiments and was added from 5 hpf onwards. For γ-secretase activity measurements, reverse-transfected CL4 cells (for Rer1p knockdown) at 60% confluency were infected with adenovirus expressing Myc-tagged NotchΔE (provided by Galapagos NV). After 48 h of transduction, the cells were treated with 10 µM lactacystin (EMD Millipore) for 5 h. The cells were lysed in Laemmli buffer, denaturated (10 min at 70°C), and separated by SDS-PAGE on 7% Tris-acetate gels (Invitrogen). c-Myc (sc789; Santa Cruz Biotechnology, Inc.) and cleaved Notch1 antibodies (Val1744; Cell Signaling Technology) were used to detect the unprocessed NotchΔE and the processed NICD, respectively.

WISH of zebrafish embryos

For in situ hybridization, two *rer1* RNA probes were produced, corresponding to the 5′ and the 3′ end of the *rer1* gene, by PCR amplification of cDNA isolated from 10-hpf wild-type embryos. As listed in Table S3, the sequences of the primers used to generate the in situ hybridization probe recognizing Rer1 1–360 bp were forward, 5′-ATGCCAGAAGGAGACAGTGC-3′, and reverse, 5′-GAAATTAATACGACTCACTATAGGCTTGAACTCTGGCAACCTCC-3′, and the one recognizing Rer1 241–585 bp were forward, 5′-GCTTTCCTCTCACCAAAAGTGG-3′, and reverse, 5′-GAAATTAATACGACTCACTATAGGAGCAAAGGTTTTCCCTGTGTCG-3′. Whole zebrafish embryos were fixed in 4% PFA for 3 h at room temperature and digested in proteinase K (concentration and incubation time depended on the embryo stage). Probes were hybridized at 65°C and detected using AP-labeled antidigoxigenin antibody (incubated overnight at 4°C) and visualized with 4-nitroblue tetrazolium/5-bromo-4-chloro-3-indolyl phosphate (Roche). Embryos were mounted in 70% glycerol and imaged using a stereomicroscope (SZX16 [Olympus] or Discovery.V8 [Carl Zeiss]).

Alcian blue staining of zebrafish embryos

For cartilage staining with Alcian blue, larvae at 6 dpf were fixed in 4% PFA for 2 h, washed with 50% ethanol, and stained with acid-free 0.4% Alcian blue solution in 70% ethanol overnight. Subsequently, larvae were bleached for 1 h using 3.5% H_2O_2 in 1% KOH and cleared in a series of glycerol solutions in KOH (20 and 50% glycerol in 0.25% KOH and 50% glycerol in 0.1% KOH).

Cilia motility assay

Embryos were dechorionated at the six- to eight-somite stage and mounted in 1% low melt agarose. 0.5–2-µm fluorescent beads (Polysciences, Inc.) were injected into the KV and imaged on a compound microscope (DMRA; Leica) using a 40× Plan Apochromat objective with a digital camera (CoolSNAP HQ; Photometrics). MetaMorph (Universal Imaging Corp.) was used to track individual beads.

Scanning and transmission EM

Samples were fixed overnight at 4°C in 0.1 M sodium-cacodylate buffer containing 2.5% glutaraldehyde and 2% PFA. After washing, they were additionally fixed for 2 h at 4°C in 1% osmium tetroxide and then rinsed with distilled water and dehydrated through a graded ethanol series. For scanning EM, fish embryos were transferred to hexamethyl disilazane for 15 min and dried overnight in a critical point dryer (CPD7501; Polaron). Mounted samples were coated with platinum, and pictures were taken using a field emission scanning electron microscope (JSM-7401F; JEOL).

For transmission EM of retina, after dehydration and en bloc staining in 4% uranyl acetate for 30 min at 4°C and after propylene oxide treatment 2 × 15 min, embryos were embedded in 100% epoxy resin for 2 d in desiccators (60°C). Transverse sections (50 µm in thickness) obtained at the optic nerve region were poststained with 4% uranyl acetate and lead citrate. Images were collected on a transmission electron microscope (JEM-2100; JEOL).

Expression analysis

For RT-PCR, 15–20 30-hpf or 30-bud eight-somite stage embryos were pooled, and total RNA was extracted (TriPure; Roche) and purified (RNeasy RNA purification columns; QIAGEN). PCR was performed using Moloney murine leukemia virus reverse transcription (RevertAid First Strand cDNA Synthesis kit; Thermo Fisher Scientific) and random hexamer primers. The sequences of the primers used for quantitative PCR were as follows Rer1 forward, 5′-TTATCAGTCCTGGCTAGACAAG-3′, and reverse, 5′-GCTCAGGCCCAGTGTCA-3′; Foxj1a forward, 5′-TACTTCCGCCACGCAGAT-3′, and reverse, 5′-GAAGCATTTGTTCAGGGACAG3′; and actin forward, 5′-TGCCCCTCGTGCTGTTTT-3′, and reverse, 5′-TCCCATGCCAACCATCACT-3′ (Table S3).

For Western blot of zebrafish tissues, 24- or 30-hpf embryos were dechorionated and deyolked in PBS followed by homogenization in lysis buffer (150 mM NaCl, 50 mM Hepes, pH 7.5, 1 mM EDTA, 1% NP-40, 0.5% Na-deoxycholate, 0.1% SDS, and protease inhibitors). For Western blots of mammalian cells, cells were harvested in PBS, centrifuged, and lysed in STE buffer (320 mM sucrose, 5 mM Tris-HCl, and 2 mM EGTA, pH 7.3) with 1% Triton X-100 and protease inhibitors. Cleared cell extracts were analyzed on 4–12% NuPAGE Bis-Tris gels in MES running buffer (Invitrogen) followed by Western blotting and immunodetection using ECL (PerkinElmer).

For Gli3 Western blots, S12 cells transfected for 72 h with siRNA for nonspecific control or siRer1 were serum starved with or without 200 ng octyl–sonic Hh for the last 24 h and then lysed in radioimmunoprecipitation assay buffer (50 mM Tris-Cl, pH 7.5, 100 mM NaCl, 1 mM EDTA, 1% Na-deoxycholate, 1% Triton X-100, and 0.1% SDS plus freshly added 1 mM PMSF and protease inhibitor tablet [Complete; Roche]) for 30 min on ice. Lysates were centrifuged at 16,000 *g* for 15 min, and 30 µg of each (determined by the bicinchoninic acid assay [Thermo Fisher Scientific]) were separated on 4–12% Tris-glycine gels (Novex) along with 5-µl molecular weight markers (SeeBlue Plus2; Invitrogen) and transferred to 0.2-µm pore nitrocellulose membranes in Tris-glycine buffer (Invitrogen) with 20% methanol and 0.01% SDS. Blots were blocked for 30 min in milk buffer (5% wt/vol milk powder and 0.1% Tween 20 in PBS) and immunostained at 4°C overnight with 3 µg/ml of mouse anti-Gli3N 6F5 (Wen et al., 2010) or 1:10,000 mouse antitubulin 1A2 (T9028; Sigma-Aldrich) in milk buffer, washed 4×, and then incubated with 1:3,000 HRP-conjugated anti–mouse for 1 h at room temperature (GE Healthcare), washed 4×, and detected with Chemiglow (for 6F5; Alpha Innotech) or ECL (for 1A2; GE Healthcare).

Antibodies

Rabbit polyclonal antibodies were generated against the C termini of mouse (CKRRYKGKEDVGKTFAS coupled to KLH; Thermo Fisher Scientific; PickCell Laboratories) or zebrafish (RTYRGKDDTGKTFAS; GenScript Corporation) Rer1p and affinity purified before use. Antibodies were used against hRer1 (J. Fuellekrug, Universitaetsklinikum, Heidelberg, Germany), acetylated tubulin (6-11B-1; Sigma-Aldrich), γ-tubulin (GTU-88; Sigma-Aldrich), tubulin (1A2; Sigma-Aldrich), F-actin (AC-15; Sigma-Aldrich), GAPDH (6C3; EMD Millipore), PC2 (G. Pazour, University of Massachusetts Medical School, Worcester, MA), polyductin (L.M. Guay-Woodford, University of Alabama, Birmingham, AL), rab8 (K. Simons, Max Plank Institute, Dresden, Germany), Arl13b (K. Kontani, University of Tokyo, Tokyo, Japan), BBS4 (Abcam), BBS7 (Abcam), Kif3a (Sigma-Aldrich), Gli3 (6F5 or 2676A; S.J. Scales), Ift88 (13967-1-AP; Proteintech), Smoothened (S.J. Scales), Zpr1 and Zpr3 (Zebrafish International Resource Center, University of Oregon, Eugene, OR), c-Myc (A-14; sc789; Santa Cruz Biotechnology, Inc.), cleaved Notch1 (Val1744; Cell Signaling Technology), N-cadherin (BD), Ift20 (Abcam), and GMAP210 (BD), HA (3F10; Roche). Details on antibody dilutions are provided in Table S5.

Immunofluorescence and confocal imaging

For immunofluorescence in zebrafish, whole embryos were fixed in 4% PFA overnight at 4°C. Primary antibodies were incubated for 3 h at room temperature, and secondary antibodies were incubated overnight at 4°C.

For immunostaining of retinal sections, zebrafish embryos (4 dpf) were fixed in 4% PFA in PBS overnight at 4°C, embedded in 1.5% agar–5% sucrose, and transferred to 30% sucrose overnight at 4°C for cryoprotection. Transverse cryosections (10 µm in thickness), cut through the midsection of the eyes, were incubated 1 h at room temperature in blocking solution (3% BSA in PBS), overnight in primary antibody diluted in PBS containing 0.3% BSA, and 1 h in secondary antibody. Finally, nuclei were stained by DAPI.

For immunofluorescence of mammalian cells, cells were fixed in 4% PFA for 20 min at room temperature or ice-cold methanol for 5 min at −20°C, permeabilized with 0.1% Triton X-100 for 10 min, blocked in

blocking buffer (2% BSA, 2% FBS, and 1% gelatin) with 5% normal goat serum for 60 min at room temperature (for CL4 cells grown on Transwell [Corning]), blocking was performed in PBS with 2% normal goat serum), incubated with the primary antibody overnight at 4°C (or overnight at 30°C when grown on Transwell), and subsequently with the Alexa Fluor–coupled secondary antibodies (Invitrogen). Slides were mounted in antifade reagent with DAPI (ProLong; Molecular Probes).

For Gli3 and Smoothened immunofluorescence staining, S12 cells grown to confluence in Lab-Tek II 8-well slides were serum starved for 16 h and treated or not treated with 200 ng/ml octyl–sonic Hh for 16 h (Smoothened) or 30 min (Gli3). Cells were then fixed in prechilled methanol for 5 min at −20°C, blocked in 2% FBS and 1% BSA in PBS for 1 h, and stained with 1:3,000 mouse anti–acetylated tubulin 6-11B-1 (T6793; Sigma-Aldrich), 1:2,300 mouse anti–γ-tubulin GTU-88 (T6557; Sigma-Aldrich), and 3 µg/ml affinity-purified rabbit anti-Smoothened (5928B; Wen et al., 2010) or 3 µg/ml affinity-purified rabbit anti-Gli3N (2676; Wen et al., 2010) in PBS. Primary antibodies were detected with highly cross-adsorbed FITC-conjugated donkey F(ab')$_2$ anti–mouse (715–096-150; Jackson ImmunoResearch Laboratories, Inc.) and Cy3-conjugated donkey F(ab')$_2$ anti–rabbit (711–166-152; Jackson ImmunoResearch Laboratories, Inc.), and coverslips (number 1.5; Corning 2940–245) were mounted in ProLong gold with DAPI (Invitrogen).

2-dpf ET4 and 30-hpf Tp1:hmgb1-mCherry transgenic embryos were dechorionated, anaesthetized in Tricaine, positioned in 1.5% low melting point agarose, and imaged by confocal microscopy. Quantification of Tp1 fluorescence was performed on a sum projection using ImageJ (National Institutes of Health).

Images were acquired on a confocal microscope (Radiance 2100; Carl Zeiss) connected to an upright microscope (Eclipse E800; Nikon) or an upright confocal microscope (SP5; Leica). Acquisition software was either LaserSharp2000 (Carl Zeiss) or LAS (Leica). Objectives used were Plan Apochromat 20×, 0.7 NA (Leica), water immersion 25×, 0.95 NA (Leica), or 40×, 0.8 NA (Nikon) and oil immersion 63×, 1.4 NA (Leica) or 60×, 1.4 NA (Nikon). Images were processed with LaserSharp2000, Photoshop (Adobe), or ImageJ and assembled in CorelDraw or Illustrator (Adobe) softwares. Cilia length measurements and image processing were performed using ImageJ or MetaMorph software. For the imaging of Gli3 and Smoothened immunofluorescence staining, slides were viewed at room temperature using a DeltaVision RT system (Applied Precision), with a microscope (1X71; Olympus) and 60× Plan Apochromat N objective NA 1.42 (Olympus) and imaged with a charge-coupled device camera (CH350; Photometrics) powered by SoftWoRx (version 3.4.4) software (Applied Precision). Figures were compiled in Photoshop CS5.1, and γ levels were adjusted on the entire panel as appropriate to ensure optimal visibility of the intended antigen.

Optokinetic response

4-dpf zebrafish larvae were immobilized in 1.5% low melting agarose. The agarose surrounding the eyes was removed. The larvae were place on a stage and exposed to alternating black and white stripes using a custom-made motorized device. Images were acquired with a camera mounted on a stereomicroscope at a frame rate of five frames/second (AxioVision; Carl Zeiss). The angle of rotation of the eye was measured manually using ImageJ.

ERG

4.5-dpf zebrafish larvae were paralyzed by injection of α-bungarotoxin (Invitrogen) in the notochord. Paralyzed larvae were positioned laterally on a wet paper towel sitting on a silver-coated wire used as reference electrode. A glass microelectrode (Narishige) with an opening of ∼20 µm and filled with PBS was placed on the center of the cornea using a motorized micromanipulator (Scientifica). A 10-ms blue light stimulus was generated by a light-emitting diode using a pulse generator, and the electrical current was measured for 1 s after the stimulus. Recorded voltages were low-pass filtered at 2 kHz, digitized at 10 kHz, and smoothened using a sliding window mean of 1 ms. The light stimulation protocol was repeated 60 consecutive times with 2.5-s intervals between the light pulses. Photovoltaic effect was measured by applying the electrode to the surface of the hindbrain and subtracted from the ERG traces. Photoreceptor response and ON bipolar response were measured by averaging the activity from 0 to 50 ms and 50 to 120 ms after the light stimulus, respectively. Data acquisition and all the analyses were performed in MATLAB (MathWorks) with custom software.

Statistical analysis

Results are expressed as means ± SEM or SD as mentioned in figure legends. Differences between means or medians were evaluated using unpaired Student's *t* test (Excel software [Microsoft]) or Wilcoxon rank sum test (MATLAB), respectively. Values of $P < 0.05$ were considered to be significant.

Online supplemental material

Fig. S1 shows the efficiency of Rer1p down-regulation in zebrafish upon MO injection. Fig. S2 shows that *rer1* down-regulation in CL4 cells does not affect the ciliary localization of proteins important for cilia biogenesis and function. Video 1 shows the response to acoustic stimuli by uninjected embryos. Video 2 shows the response to acoustic stimuli by Rer1p morphants. Video 3 shows fluid flow in KV of uninjected embryos. Video 4 shows fluid flow in KV of Rer1p morphants. Table S1 shows the overview of cell lines used in this study. Table S2 shows a summary of siRNA sequences. Table S3 shows a list of primers used in this study. Table S4 shows sequences of MOs. Table S5 shows the overview and dilution of antibodies used for immunofluorescence and Western blotting. Online supplemental material is available at http://www.jcb.org/cgi/content/full/jcb.201208175/DC1.

The authors thank the VIB Bio Imaging core (Light Microscopy and Imaging Network and Electron Microscopy and Imaging Network), the zebrafish community for in situ probes, and S. Louwette (KULeuven) for technical expertise. We are grateful to J. Füllekrug, G. Pazour, L.M. Guay-Woodford, K. Simons, and K. Kontani for antibodies and constructs and H. Lopez-Schier, M. Parsons, and L. Bally-Cuif for transgenic ET4 and TP1:hmgb1-mCherry fish. We thank I. Drummond for critical reading.

This work was financially supported by grants to W. Anneart from the KULeuven (GOA/11/009), the Fonds Wetenschappelijk Onderzoek (G.0.708.10), the Stichting Alzheimer Onderzoek-Fondation Recherche Alzheimer (S#12012), Hercules Foundation (AKUL/09/037 and AKUL/11/30), and the federal government (IAP P7/16). N. Jurisch-Yaksi held an F+ fellowship (KULeuven). Support for C.B. Arrington was provided a National Institute of Child Health and Human Development grant (K08HD062638). S.J. Scales is an employee of Genentech.

Submitted: 30 August 2012
Accepted: 11 February 2013

References

Daudet, N., and J. Lewis. 2005. Two contrasting roles for Notch activity in chick inner ear development: specification of prosensory patches and lateral inhibition of hair-cell differentiation. *Development*. 132:541–551. http://dx.doi.org/10.1242/dev.01589

De Strooper, B., and W. Annaert. 2010. Novel research horizons for presenilins and γ-secretases in cell biology and disease. *Annu. Rev. Cell Dev. Biol.* 26:235–260. http://dx.doi.org/10.1146/annurev-cellbio-100109-104117

De Strooper, B., W. Annaert, P. Cupers, P. Saftig, K. Craessaerts, J.S. Mumm, E.H. Schroeter, V. Schrijvers, M.S. Wolfe, W.J. Ray, et al. 1999. A presenilin-1-dependent gamma-secretase-like protease mediates release of Notch intracellular domain. *Nature*. 398:518–522. http://dx.doi.org/10.1038/19083

Eggenschwiler, J.T., and K.V. Anderson. 2007. Cilia and developmental signaling. *Annu. Rev. Cell Dev. Biol.* 23:345–373. http://dx.doi.org/10.1146/annurev.cellbio.23.090506.123249

Ellgaard, L., and A. Helenius. 2003. Quality control in the endoplasmic reticulum. *Nat. Rev. Mol. Cell Biol.* 4:181–191. http://dx.doi.org/10.1038/nrm1052

Essner, J.J., J.D. Amack, M.K. Nyholm, E.B. Harris, and H.J. Yost. 2005. Kupffer's vesicle is a ciliated organ of asymmetry in the zebrafish embryo that initiates left-right development of the brain, heart and gut. *Development*. 132:1247–1260. http://dx.doi.org/10.1242/dev.01663

Evangelista, M., T.Y. Lim, J. Lee, L. Parker, A. Ashique, A.S. Peterson, W. Ye, D.P. Davis, and F.J. de Sauvage. 2008. Kinome siRNA screen identifies regulators of ciliogenesis and hedgehog signal transduction. *Sci. Signal.* 1:ra7. http://dx.doi.org/10.1126/scisignal.1162925

Feng, S., A. Knödler, J. Ren, J. Zhang, X. Zhang, Y. Hong, S. Huang, J. Peränen, and W. Guo. 2012. A Rab8 guanine nucleotide exchange factor-effector interaction network regulates primary ciliogenesis. *J. Biol. Chem.* 287:15602–15609. http://dx.doi.org/10.1074/jbc.M111.333245

Frank-Kamenetsky, M., X.M. Zhang, S. Bottega, O. Guicherit, H. Wichterle, H. Dudek, D. Bumcrot, F.Y. Wang, S. Jones, J. Shulok, et al. 2002. Small-molecule modulators of Hedgehog signaling: identification and characterization of Smoothened agonists and antagonists. *J. Biol.* 1:10. http://dx.doi.org/10.1186/1475-4924-1-10

Haddon, C., Y.J. Jiang, L. Smithers, and J. Lewis. 1998. Delta-Notch signalling and the patterning of sensory cell differentiation in the zebrafish ear: evidence from the mind bomb mutant. *Development*. 125:4637–4644.

He, Q., G. Wang, S. Dasgupta, M. Dinkins, G. Zhu, and E. Bieberich. 2012. Characterization of an apical ceramide-enriched compartment regulating ciliogenesis. *Mol. Biol. Cell*. 23:3156–3166. http://dx.doi.org/10.1091/mbc.E12-02-0079

Huangfu, D., A. Liu, A.S. Rakeman, N.S. Murcia, L. Niswander, and K.V. Anderson. 2003. Hedgehog signalling in the mouse requires intraflagellar transport proteins. *Nature*. 426:83–87. http://dx.doi.org/10.1038/nature02061

Ishikawa, H., and W.F. Marshall. 2011. Ciliogenesis: building the cell's antenna. *Nat. Rev. Mol. Cell Biol.* 12:222–234. http://dx.doi.org/10.1038/nrm3085

Kaimori, J.Y., Y. Nagasawa, L.F. Menezes, M.A. Garcia-Gonzalez, J. Deng, E. Imai, L.F. Onuchic, L.M. Guay-Woodford, and G.G. Germino. 2007. Polyductin undergoes notch-like processing and regulated release from primary cilia. *Hum. Mol. Genet.* 16:942–956. http://dx.doi.org/10.1093/hmg/ddm039

Kopan, R., and M.X. Ilagan. 2009. The canonical Notch signaling pathway: unfolding the activation mechanism. *Cell*. 137:216–233. http://dx.doi.org/10.1016/j.cell.2009.03.045

Kramer-Zucker, A.G., F. Olale, C.J. Haycraft, B.K. Yoder, A.F. Schier, and I.A. Drummond. 2005. Cilia-driven fluid flow in the zebrafish pronephros, brain and Kupffer's vesicle is required for normal organogenesis. *Development*. 132:1907–1921. http://dx.doi.org/10.1242/dev.01772

Lai, C.K., N. Gupta, X. Wen, L. Rangell, B. Chih, A.S. Peterson, J.F. Bazan, L. Li, and S.J. Scales. 2011. Functional characterization of putative cilia genes by high-content analysis. *Mol. Biol. Cell*. 22:1104–1119. http://dx.doi.org/10.1091/mbc.E10-07-0596

Lopes, S.S., R. Lourenço, L. Pacheco, N. Moreno, J. Kreiling, and L. Saúde. 2010. Notch signalling regulates left-right asymmetry through ciliary length control. *Development*. 137:3625–3632. http://dx.doi.org/10.1242/dev.054452

Nauli, S.M., F.J. Alenghat, Y. Luo, E. Williams, P. Vassilev, X. Li, A.E. Elia, W. Lu, E.M. Brown, S.J. Quinn, et al. 2003. Polycystins 1 and 2 mediate mechanosensation in the primary cilium of kidney cells. *Nat. Genet.* 33:129–137. http://dx.doi.org/10.1038/ng1076

Nigg, E.A., and J.W. Raff. 2009. Centrioles, centrosomes, and cilia in health and disease. *Cell*. 139:663–678. http://dx.doi.org/10.1016/j.cell.2009.10.036

Omori, Y., C. Zhao, A. Saras, S. Mukhopadhyay, W. Kim, T. Furukawa, P. Sengupta, A. Veraksa, and J. Malicki. 2008. Elipsa is an early determinant of ciliogenesis that links the IFT particle to membrane-associated small GTPase Rab8. *Nat. Cell Biol.* 10:437–444. http://dx.doi.org/10.1038/ncb1706

Parinov, S., I. Kondrichin, V. Korzh, and A. Emelyanov. 2004. Tol2 transposon-mediated enhancer trap to identify developmentally regulated zebrafish genes in vivo. *Dev. Dyn.* 231:449–459. http://dx.doi.org/10.1002/dvdy.20157

Parsons, M.J., H. Pisharath, S. Yusuff, J.C. Moore, A.F. Siekmann, N. Lawson, and S.D. Leach. 2009. Notch-responsive cells initiate the secondary transition in larval zebrafish pancreas. *Mech. Dev.* 126:898–912. http://dx.doi.org/10.1016/j.mod.2009.07.002

Pazour, G.J., J.T. San Agustin, J.A. Follit, J.L. Rosenbaum, and G.B. Witman. 2002. Polycystin-2 localizes to kidney cilia and the ciliary level is elevated in orpk mice with polycystic kidney disease. *Curr. Biol.* 12:R378–R380. http://dx.doi.org/10.1016/S0960-9822(02)00877-1

Raya, A., Y. Kawakami, C. Rodriguez-Esteban, D. Buscher, C.M. Koth, T. Itoh, M. Morita, R.M. Raya, I. Dubova, J.G. Bessa, et al. 2003. Notch activity induces Nodal expression and mediates the establishment of left-right asymmetry in vertebrate embryos. *Genes Dev.* 17:1213–1218. http://dx.doi.org/10.1101/gad.1084403

Sato, M., K. Sato, and A. Nakano. 2004. Endoplasmic reticulum quality control of unassembled iron transporter depends on Rer1p-mediated retrieval from the golgi. *Mol. Biol. Cell*. 15:1417–1424. http://dx.doi.org/10.1091/mbc.E03-10-0765

Shearman, M.S., D. Beher, E.E. Clarke, H.D. Lewis, T. Harrison, P. Hunt, A. Nadin, A.L. Smith, G. Stevenson, and J.L. Castro. 2000. L-685,458, an aspartyl protease transition state mimic, is a potent inhibitor of amyloid beta-protein precursor gamma-secretase activity. *Biochemistry*. 39:8698–8704. http://dx.doi.org/10.1021/bi0005456

Sidi, S., R.W. Friedrich, and T. Nicolson. 2003. NompC TRP channel required for vertebrate sensory hair cell mechanotransduction. *Science*. 301:96–99. http://dx.doi.org/10.1126/science.1084370

Spasic, D., T. Raemaekers, K. Dillen, I. Declerck, V. Baert, L. Serneels, J. Füllekrug, and W. Annaert. 2007. Rer1p competes with APH-1 for binding to nicastrin and regulates γ-secretase complex assembly in the early secretory pathway. *J. Cell Biol.* 176:629–640. http://dx.doi.org/10.1083/jcb.200609180

Valkova, C., M. Albrizio, I.V. Röder, M. Schwake, R. Betto, R. Rudolf, and C. Kaether. 2011. Sorting receptor Rer1 controls surface expression of muscle acetylcholine receptors by ER retention of unassembled alpha-subunits. *Proc. Natl. Acad. Sci. USA*. 108:621–625. http://dx.doi.org/10.1073/pnas.1001624108

Wen, X., C.K. Lai, M. Evangelista, J.A. Hongo, F.J. de Sauvage, and S.J. Scales. 2010. Kinetics of hedgehog-dependent full-length Gli3 accumulation in primary cilia and subsequent degradation. *Mol. Cell. Biol.* 30:1910–1922. http://dx.doi.org/10.1128/MCB.01089-09

Whitfield, T.T., B.B. Riley, M.Y. Chiang, and B. Phillips. 2002. Development of the zebrafish inner ear. *Dev. Dyn.* 223:427–458. http://dx.doi.org/10.1002/dvdy.10073

Yu, X., C.P. Ng, H. Habacher, and S. Roy. 2008. Foxj1 transcription factors are master regulators of the motile ciliogenic program. *Nat. Genet.* 40:1445–1453. http://dx.doi.org/10.1038/ng.263

Zaghloul, N.A., and S.A. Brugmann. 2011. The emerging face of primary cilia. *Genesis*. 49:231–246. http://dx.doi.org/10.1002/dvg.20728